

## INVESTIGATION OF THE FERMI SURFACE OF INDIUM

R. T. MINA and M. S. KHAÏKIN

Institute for Physics Problems, Academy of Sciences U.S.S.R., Physics Institute,  
State Atomic Energy Commission

Submitted to JETP editor July 20, 1964; resubmitted October 2, 1964

J. Exptl. Theoret. Phys. (U.S.S.R.) 48, 111-121 (January, 1965)

The effective masses of the current carriers in indium were measured by the cyclotron resonance method, and their anisotropy in the (010), (001) and (111) planes was studied. The extremal dimensions of the hole Fermi surface were determined by the cyclotron resonance cut-off method. The experimental results are discussed and compared with the model of the Fermi surface for indium. Some features of Fermi surfaces of metals with similar crystal structures (lead, aluminum, indium) resulting from differences in the parameters of these metals are compared.

THE tetragonal face-centered crystal lattice of indium with ratio of lattice constants  $c/a = 1.08$  can be regarded as a cubic face-centered lattice somewhat elongated along the [001] direction; such a lattice is characteristic of aluminum and lead. Therefore, it can be expected that the Fermi surfaces are similar to the energy surfaces of aluminum and lead, which have been well studied. However, the slight compression of the Brillouin zone along the [001] axis must lead to interesting differences from the viewpoint of the effect of the lattice potential on the energy spectrum of the current carriers. The absence of detailed investigations of the Fermi surface of indium, in particular by the cyclotron resonance method (there exists only a brief note<sup>[1]</sup> on the discovery of this effect), stimulated the present research.

Single crystals of indium were prepared for the investigation in the form of discs of diameter 17.8 mm; three specimens had a thickness of 1 mm and the fourth specimen a thickness of 0.31 mm. The single crystal was placed in a strip-resonator tuned to a frequency of 18.7 Gc. The magnetic field was applied parallel to the plane surface of the specimen and was rotated in this plane. The reactive part of the surface impedance of the metal was measured by the frequency modulation method.<sup>[2]</sup>

Examples of recordings of cyclotron resonance are shown in Figs. 1 and 2. In the first of these, two series of cyclotron resonances having different periods are clearly evident. The effective masses were determined from such spectra by the formula  $\mu = m^*/m_0 = H_{\text{epr}}^{-1}/\Delta H^{-1}$  [Eq. (1) in<sup>[3]</sup>], where  $\Delta H^{-1}$  is the period of cyclotron

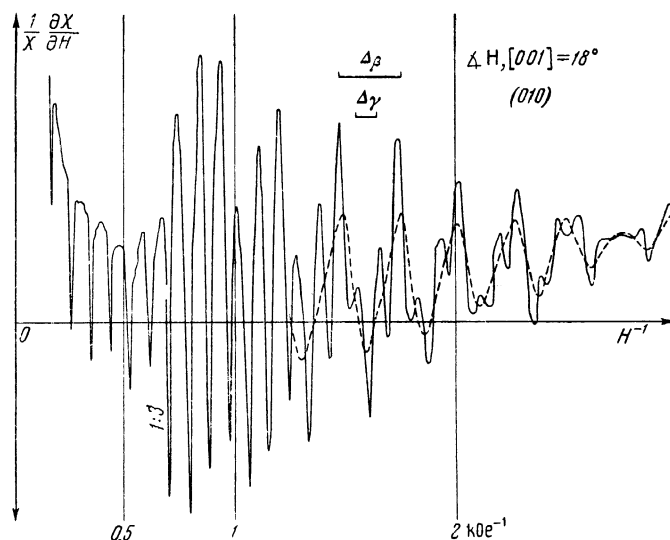


FIG. 1. Recording of the logarithmic derivative of the reactive part of the surface impedance of indium as a function of the reciprocal of the magnetic field  $H^{-1}$ . The orientation of the surface of the sample and the field are shown on the upper right. The lengths  $\Delta\beta$  and  $\Delta\gamma$  are the periods of the cyclotron resonances, measured from this recording. The location of change of amplification of the circuit by a factor of three is indicated by the symbol 1:3.

resonances as a function of the inverse field,  $H_{\text{epr}}$  is the value of the magnetic field of electron paramagnetic resonance.

Three crystallographic planes were studied: (001), (010), (111). In the first two planes, two groups of effective masses were observed, differing by a factor of more than three. In the last, only effective masses of lower value were observed, evidently connected with some imperfection in the specimen. The resistance ratio meas-

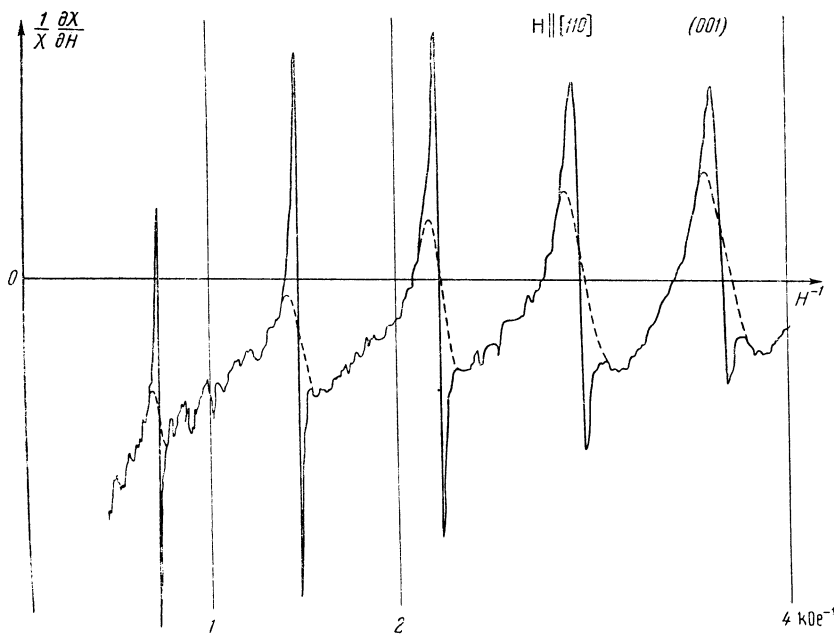


FIG. 2. Recording of the cyclotron resonance on the tubes  $\beta$  of the electron Fermi surface of indium.

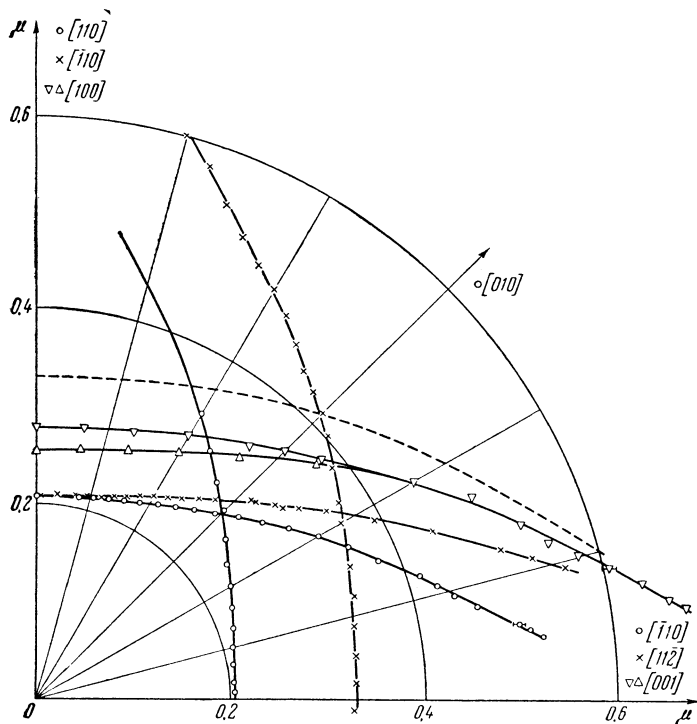


FIG. 3. Anisotropy of the effective masses of the electrons in indium. The symbols correspond to masses measured with rotation of the field in the planes:  $\circ$  - (001),  $\times$  - (111) and  $\nabla$  - (010). The directions of the axes corresponding to these planes are shown in the drawing by the same signs. The dashed line is the bisector of the diagram of experimental curve denoted by the crosses selected relative to the experimental curve denoted by the crosses mirrored in the bisector of the diagram (for convenience in comparison).

ured in this specimen<sup>1)</sup> amounted to  $\rho(300^\circ\text{K})/\rho(4.2^\circ\text{K}) = 15,500$ .

#### EFFECTIVE MASSES OF THE ELECTRONS

The set of effective masses observed in the three different crystallographic planes and plotted

<sup>1)</sup>This measurement was made by V. S. Tsoř, to whom the authors express their gratitude.

in the polar diagram of Fig. 3 correspond to an energy surface consisting of two tubes, the axes of which are directed along the crystallographic directions  $[110]$  and  $[\bar{1}10]$ . Because of the fact that the plane of one of the specimens is inclined at an angle of  $4^\circ$  to the plane of symmetry (010), it was possible to observe cyclotron resonance on each of the tubes separately, as is seen in Fig. 3.

The strong departure of the graphs of the effective masses in the polar diagram of Fig. 3

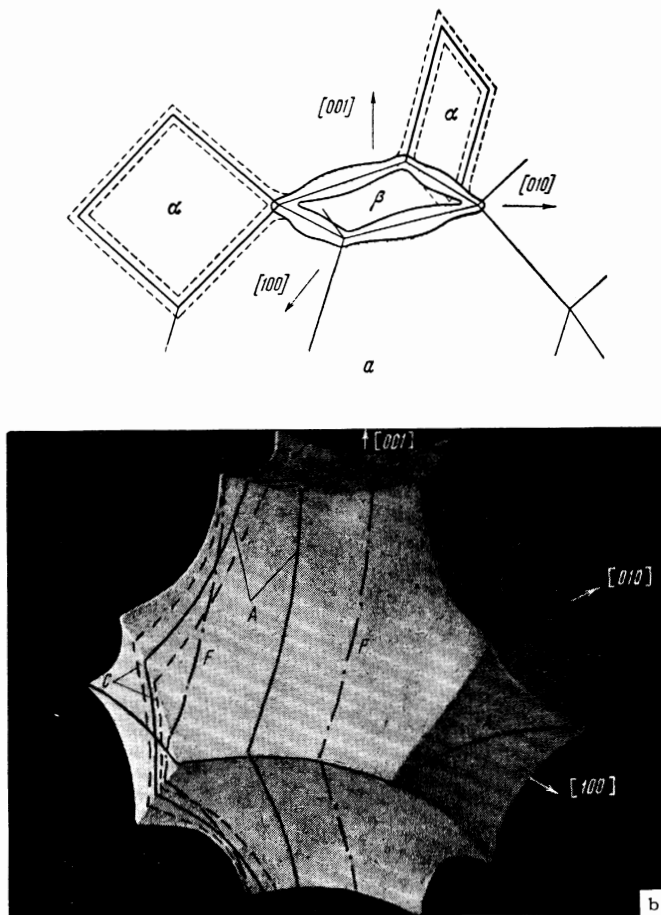


FIG. 4. Model of the Fermi surface of indium in the approximation of nearly free electrons: a – electron surface of the third zone, b – hole surface of the second zone.

from straight lines at large angles of rotation of the field relative to the  $[110]$  axis shows that the tubes, which are cylindrical in the central portion, narrow at the ends in contrast to the situation which prevails for lead.<sup>[3]</sup>

One can see in Fig. 2 that the lines of cyclotron resonance have a complicated form on the tube for  $H \parallel [110]$ . In addition to the narrow resonance peaks, the periodicity of which corresponds to a mass  $\mu = 0.208$ , an almost sinusoidal curve is clearly evident (part of it is shown as a dotted line in Fig. 2), the period of which corresponds to a mass  $\mu' = 0.18$ . One can explain the detailed shape of the line by the fact that the tube which tapers at its ends has two extremal cross sections: the larger mass  $\mu$  corresponds to the maximum cross section of the tube at its middle, almost cylindrical part, while the smaller mass  $\mu'$  corresponds to the two minimal cross sections close to the ends of the tube.

The increase in the effective mass after the

minimal cross section is reasonably explained by the effect of the ends of the mutually perpendicular tubes  $[110]$  and  $[\bar{1}10]$ . Rotation of the field in the  $(001)$  plane by  $50^\circ$ – $60^\circ$  from the  $[110]$  axis leads to the disappearance of the difference of the masses  $\mu$  and  $\mu'$  (see, for example, Fig. 1).

Returning to the model of the Fermi surface constructed in the approximation of nearly free electrons (Fig. 4), it is not difficult to see that the effective masses determined in the experiment correspond to an electron surface composed of the tubes  $\beta$ . According to this model, there must also exist much thinner tubes  $\alpha$  along the four axes which are equivalent to  $[101]$ . However, no data were obtained on their existence in this research. In the range of rotation of the field by more than  $160^\circ$  in the  $(010)$  plane, the amplitude of cyclotron resonance corresponding to the tubes  $\beta$  decreases in comparison with its maximum value by a factor of 50, after which it vanishes in the noise. At the same time, if the amplitude of the resonance of  $\alpha$  had exceeded the noise level by a factor of 5, then this resonance would have been discovered. Therefore one can confirm the fact that the amplitude of the resonance corresponding to the tube  $\alpha$ , if it exists, is at least an order of magnitude smaller than the resonance corresponding to the tube  $\beta$ .

The large range of angles in which resonance is observed in tube  $\beta$  and the character of the change in the effective mass for directions of the magnetic field almost perpendicular to the axis of tube  $\beta$  also gives evidence as to the impossibility of the existence of tubes  $\alpha$  connecting with tubes  $\beta$  in the vertices of the Brillouin zone (Fig. 4 a). Actually, if the tubes  $\alpha$ , lying in the orthogonal planes  $(100)$  and  $(010)$  (Fig. 4 a), were connected together at the point of juncture of the tubes  $\beta$  which lie in the  $(001)$  plane, then the values of the effective masses would have approached the same limit, independent of the plane in which the direction of the magnetic field approaches the  $(110)$  plane. However, it is evident from Fig. 3 that this is not so: the effective mass increases much more slowly upon rotation of the magnetic field in the  $(001)$  plane of juncture of the tubes  $\beta$  than in any other plane.

The value of the effective mass  $\mu = 0.208 \pm 0.002$  for a direction of the field along the  $[110]$  axis agrees completely with the results obtained in<sup>[4]</sup> from the temperature dependence of the quantum oscillations for the value  $\mu = 0.19$  (the accuracy of this relation amounts to approximately 10–15%).

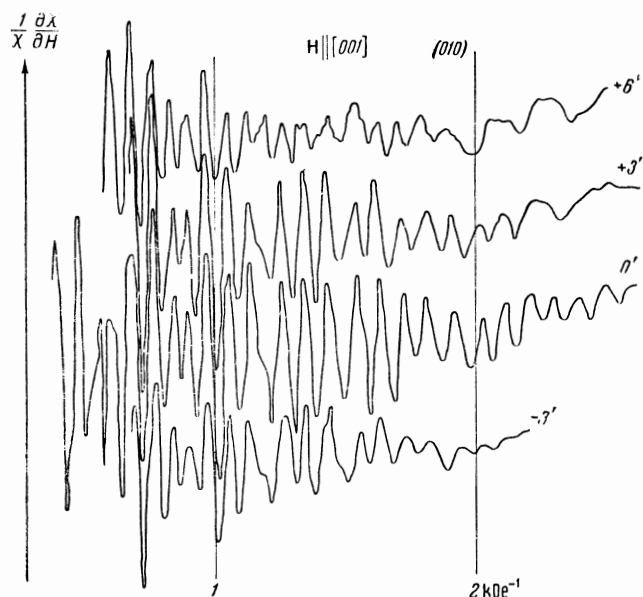


FIG. 5. Recording of the cyclotron resonances on the hole Fermi surface of indium for different angles of inclination of the field to the surface of the specimen. The angle of inclination is shown to the right of the curves.

EFFECTIVE MASSES OF HOLES

A very interesting series of cyclotron resonances was observed in the same experiments, when the magnetic field made small angles with the [100] axis (see Fig. 8 below), as well as with the axes [010] and [001] (Fig. 1). Usually resonances could be observed whose order amounted to 15-20 and sometimes to 30. The intensity of these resonances falls off sharply upon approach of the direction of the field to the crystallographic axes; in this case it becomes very sensitive to the direction of the magnetic field relative to the surface of the specimen. Thus an inclination of 15'-20' decreases the amplitude of resonance of the lower orders by a factor of almost 10. Recordings are shown in Fig. 5 of cyclotron resonances for magnetic field inclinations 3'-6' to this field of the specimen. The anisotropy of the effective masses corresponding to these cyclotron resonances is shown in Fig. 6 and below in

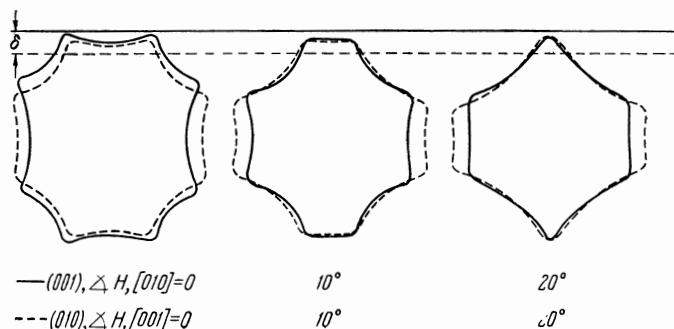


FIG. 7. Shape of the central orbits A of holes according to the model of the Fermi surface of indium for different directions of the field, as shown above.

Fig. 9.

According to the nearly free electron model, the hole Fermi surface of indium in the second zone has the shape shown in Fig. 4 b. Its dimensions exceed by a factor of 4-5 the diameter of the tubes of which the electron surface of the third zone is composed. In its fundamental characteristics, it is similar to the hole surface of aluminum<sup>[5,6]</sup> and to the very smooth hole surface of lead.<sup>[3]</sup> As is also the case with aluminum and lead, the effective mass corresponding to a central orbit decreases upon departure of the field direction from the [100], [010], and [001] axes, while the amplitude of the cyclotron resonance increases. According to calculations made with the model of the energy surface of aluminum,<sup>[6]</sup> resonance on the noncentral orbits C and F is possible, in addition to resonance on the central orbit A (Fig. 4 b). The effective masses of A, C, and F observed in the experiment (Figs. 6 and 9) refer to the corresponding orbits on the hole surface in Fig. 4 b.

Figure 7 shows the shape of the central orbits A for holes, which are constructed on the Fermi surface model for different directions of the magnetic field. Such changes in the shape of the orbit upon rotation of the field lead to a decrease in the time that the hole stays in the skin layer  $\delta$  and consequently to a decrease in the intensity of the resonance. The angular ranges for the existence of resonance A, found from the Fermi sur-

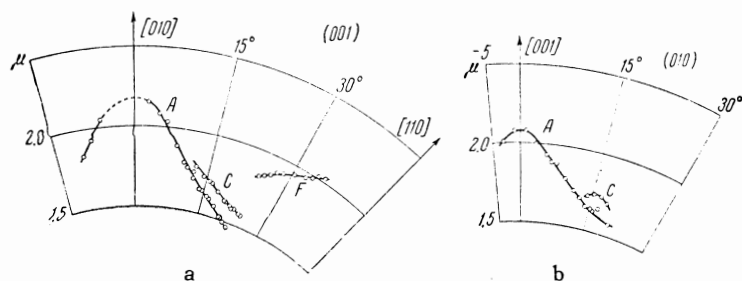


FIG. 6. Anisotropy of the effective masses of holes in indium: a - in the (001) plane; b - in the (010) plane.

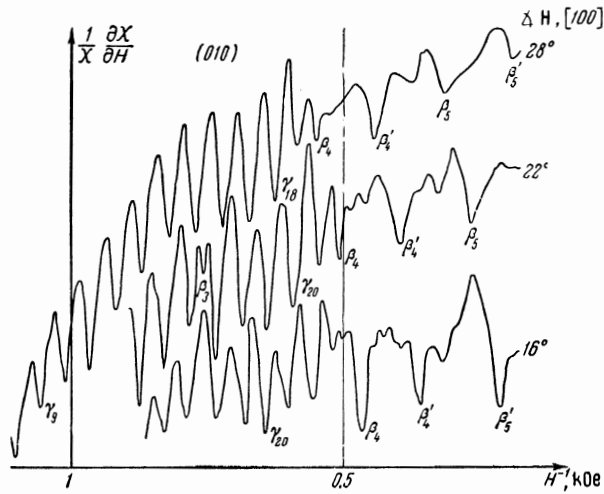


FIG. 8. Recording of the cutoff of the cyclotron resonances on the hole Fermi surface of indium for three different directions of the magnetic field in the (010) plane.  $\beta$ ,  $\beta'$  cyclotron resonances on the electron surface,  $\gamma$  on the hole surface; the index denotes the order of the resonance.

face model, amount to:  $24^\circ$  from the [010] axis in the (001) plane, and  $22^\circ$  from the [001] axis in the (010) plane. This is in excellent agreement with the corresponding values of  $23^\circ$  and  $21^\circ$ , which follow from Fig. 6. The agreement of the observed angular range of existence of the resonance A, which is equal to  $30^\circ$  in the (010) plane for rotation of the field from the [100] axis, with the value which follows from the model is graphically illustrated in Fig. 9 shown below.

As is seen from Fig. 4 b, a significant part of the orbit A, for  $\mathbf{H} \parallel [001]$ , and also for  $\mathbf{H} \parallel [010]$ , lies in the parts of the Fermi surface that have a large curvature. Upon rotation of the field, the orbit A is displaced into a region of the surface which has small curvature. Therefore, the number of holes which make a contribution to the cyclotron resonance A increases and the intensity of the latter rises appreciably. The explanation that has been given applies in full measure to the observations of similar characteristics of cyclotron resonance in lead [3] and aluminum. [6]

### THE MOMENTUM OF THE HOLES

The method of cutting off cyclotron resonances, [7,8] in contrast with methods of ultrasonic attenuation [9] and the size effects, [10] makes it possible to measure simultaneously the momentum  $p$  and the effective mass  $\mu$  of the current carriers in the metal. Results are set forth below that were obtained in experiments on a single crystal of indium having a thickness  $0.310 \pm 0.005$  mm. The angle between the plane surface

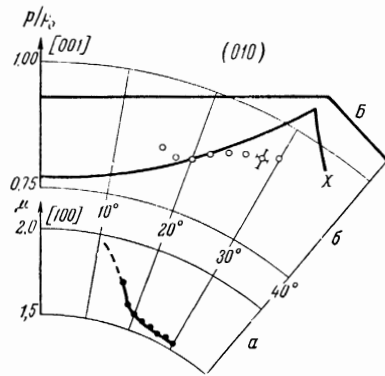


FIG. 9. Anisotropy of the effective mass  $\mu$  in the (010) plane for directions of the magnetic field close to the crystallographic axis [100] and the extremal dimensions of the central orbit  $p/p_0$  in the direction perpendicular to the magnetic field and normal to the surface of the specimen. The solid heavy lines denote the shape of the Brillouin zone B and the hole surface of the model of nearly free electrons X. The region around one of the points indicates the accuracy of the measurements.

of the specimen and the crystallographic plane (010) amounted to approximately  $4^\circ$ .

The extremal dimension of the orbit of the current carrier can be determined in momentum space according to the value of the cyclotron resonance cutoff field  $H_{\text{cut}}$  by the formula [7]

$$p/p_0 = aeDH_{\text{cut}}/2ch,$$

where  $p_0 = h/a$ ,  $a$  being the lattice constant of indium.

A recording of the cyclotron resonance cutoff is reproduced in Fig. 8 for three directions of the field, close to the [100] axis. The values of  $p/p_0$  and  $\mu$  are shown in Fig. 9. The contours of the Brillouin zone B and the hole surface X, constructed in the approximation of nearly free electrons, are also shown in this drawing.

The simultaneous measurement of the momentum and the mass of the holes allows us to calculate the mean velocity of their motion along the orbit (Eq. (5) from [7]):

$$v = D\omega / 2nH_{\text{cut}},$$

where  $n$  is a continuous function which assumes integer values at the resonance directions of the magnetic field, and  $\omega$  is the angular frequency of the electromagnetic field. The velocity, which is found from this formula for  $\times \mathbf{H}$ , [100] =  $20^\circ$ , amounted to  $v = 0.85 \times 10^8$  cm/sec. Taking into account the deviation of the shape of the orbit from a circle can change this value by  $\sim 10\%$ .

The values of the extremal diameter obtained by the method of cyclotron resonance cutoff agree

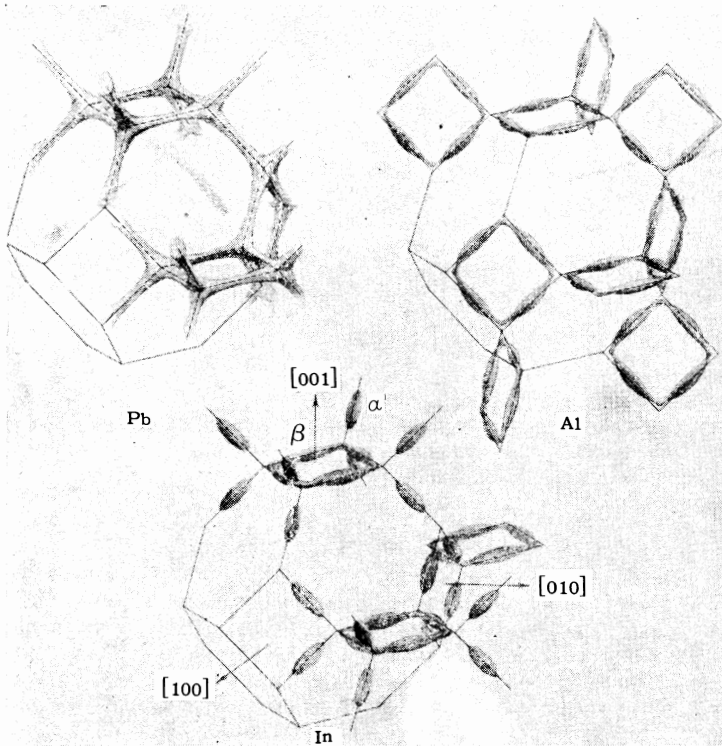


FIG. 10. Electron Fermi surfaces of the third zones of lead, aluminum and indium. For greater clarity in the drawing, the tubes of the lead surface are thinned.<sup>2)</sup>

with the results of the measurement of the size effect within the limits of error of the experiment.<sup>[10]</sup> Some systematic deviation can be explained by the difference in orientation of the specimens. The diameter of the orbit measured by the magneto-acoustic method<sup>[9]</sup> in the range  $16^\circ < \chi H$ ,  $[001] < 22^\circ$  in the (010) plane (Fig. 4 a in<sup>[9]</sup>), also agrees within the limits of experimental error with the measurements of the present research. However, in the range  $22^\circ < \chi H$ ,  $[001] < 35^\circ$ , the diameter measured in<sup>[9]</sup> decreases one and a half times and differs sharply from the values shown in Fig. 9. The reason for such a large divergence is not clear. It is possi-

bly connected with the fact that the oscillations in the ultrasonic absorption observed in this range of angles are associated with a different size of orbit, having a complicated shape.

#### COMPARISON OF THE FERMI SURFACES OF LEAD, ALUMINUM, AND INDIUM

It follows from the results of the experimental investigation of current carriers in indium set forth above that the model of the Fermi surface of indium constructed in the approximation of nearly free electrons is in excellent agreement both with the behavior of the effective masses of the current

	Direction	Period of the lattice	Valence	$P_c/P_0$	Electron tubes of the third zone			Hole surface of the second zone	
					$F$	measured cross section $(2\pi/a)^2$	cross section from the model $(2\pi/a^2)$	central orbit $\mu$	correction of the directed field*
Pb	$\langle 100 \rangle$	4.94	4	1.24	0.55 <sup>[3,15]</sup>	0.11 <sup>[13]</sup>	0.16	1.60 <sup>[3]</sup>	$\vartheta = 5^\circ$ $\varphi = 8^\circ$ $\varphi = 2^\circ$
Al	$\langle 100 \rangle$	4.04	3	1.13	0.13 <sup>[5]</sup> 0.14 <sup>[14]</sup>	0.0115 <sup>[11]</sup>	0.022	1.59 <sup>[6]</sup> , 1.9 <sup>[6]</sup> 2.0; 2, 3 <sup>[6]</sup>	
In	$\begin{cases} [100], [010] \\ [001] \end{cases}$	4.58 4.94	3 3	1.10 1.18	— 0.21	0.024 <sup>[4]</sup> 0.023 <sup>[4]</sup>	0.015 ( $\alpha$ ) 0.042 ( $\beta$ )	2.16 2.07	

\* $\vartheta = \chi H$ , [010] in the (101) plane,  $\varphi = \chi H$ , [010] in the (001) plane.

<sup>2)</sup>This drawing was made by V. P. Vol'skii, to whom the authors express their appreciation.

carriers and also with the absolute values of their momentum. A similar situation also holds for a number of other metals, in particular for lead<sup>[3]</sup> and aluminum.<sup>[6]</sup>

Let us compare some features of the electron Fermi surfaces of lead, aluminum and indium, as shown in Fig. 10. In the Table are given the radii of the spheres of free electrons in momentum space  $p_C$  relative to the average dimension of the Brillouin zone,  $p_0$ . For lead, which has the largest  $p_C/p_0$  ratio, the multiply-connected electron surface of the third zone is formed by identical tubes, the axes of which serve as the edges of the Brillouin zone  $\langle 110 \rangle$ . The tubes widen at the ends and are joined in sets of four at the vertices of the zone.<sup>[3]</sup> For aluminum, for which the parameter  $p_C/p_0$  is less, the Fermi electron surface consists of very thin tubes which become narrower at the ends and are joined in pairs near the vertices of the zone.<sup>[11]</sup> Thus the changes of the Fermi electron surface of the cubic face-centered metal in the third zone, brought about by change in the parameter  $p_C/p_0$ , can be correctly described in the approximation of nearly free electrons and geometrically represented by the method set forth in<sup>[12]</sup>.

Indium has a tetragonal face-centered lattice for which the parameter  $p_C/p_0$  in the [100] and [010] directions is less than for aluminum and has an intermediate value relative to aluminum and lead in the [001] direction. From the point of view of the approximation of nearly free electrons, this should lead to the result that the tubes  $\alpha$ , which form the electron surface of indium and which lie in the (100) and (010) planes, should be thinner than for aluminum, while the tubes  $\beta$  which lie in the (001) plane should have intermediate dimensions relative to the tubes of the Fermi surfaces of aluminum and lead. These conclusions are qualitatively supported by the present research: the electron Fermi surface of indium consists of pairwise-connected tubes  $\beta$ , while the tubes  $\alpha$  are lacking (Fig. 4 a).

In the Table are shown the areas of the central extremal cross sections of the tubes and the corresponding effective masses; it is seen that these quantities follow from changes in the parameter  $p_C/p_0$ . It is necessary to note that the transverse dimensions of the tubes of the model are determined by the quantity  $p_C/p_0 - 1$  (see, for example, Fig. 9), which makes the electron surface of the third zone especially sensitive to the parameter  $p_C/p_0$ .

Several cross sections measured in<sup>[4]</sup> pertain to tubes  $\alpha$ . Their values for the different direc-

tions of the field differ by not more than  $\sim 1.7$  times and consequently the transverse cross sections differ by  $\lesssim 30\%$ . The region of observation of the  $\alpha$  cross sections in the (001) plane is much greater than for the  $\beta$  cross sections ( $\sim 60^\circ$ ) and reaches  $90^\circ$ .<sup>[4]</sup> This compels us to think that the observed cross sections  $\alpha$  refer to almost isotropic closed portions of the Fermi surface, which are evidently deformed "remnants" of the tubes  $\alpha$  separated from the tubes  $\beta$  (Fig. 10).

The comparison of the data on the hole Fermi surfaces of the second zone of the metal under consideration is less significant, inasmuch as the dimensions of the hole surface are determined by the quantity  $2 - p_C/p_0$  and consequently are less sensitive to changes in the parameter  $p_C/p_0$  than the dimensions of the electron surface. Nevertheless, as is seen from the Table, the effective masses of the holes of the central cross section fall off with increase in the parameter  $p_C/p_0$ , as is to be expected according to the model. Unfortunately, the data on aluminum are insufficiently decisive; however, the results obtained in<sup>[5,6]</sup> give us a basis for supposing that the effective mass of the holes in aluminum has a value intermediate between the effective masses of the holes in indium and lead.

Thus the approximation of nearly free electrons not only gives a valid representation on the Fermi surface of each individual metal, but as a rule describes the changes in the Fermi surface brought about by the different parameters of the metals.

The authors are grateful to P. L. Kapitza for constant attention and interest in the work, to G. S. Chernyshev and V. A. Yudin for technical assistance.

<sup>1</sup>Castle, Chandrasekhar, and Rayne, Phys. Rev. Lett. 6, 409 (1961).

<sup>2</sup>M. S. Khaikin, PTÉ, No. 3, 95 (1961).

<sup>3</sup>R. T. Mina and M. S. Khaikin, JETP 45, 1304 (1963), Soviet Phys. JETP 18, 876 (1963).

<sup>4</sup>G. B. Brandt, and J. A. Rayne, Phys. Rev. 132, 1512 (1963); Phys. Rev. Lett. 12, 87 (1964).

<sup>5</sup>T. W. Moor, F. W. Spong, Phys. Rev. 125, 846 (1962).

<sup>6</sup>V. P. Naberezhnykh and V. P. Tolstoluzhskii, JETP 46, 18 (1964), Soviet Phys. JETP 19, 13 (1964).

<sup>7</sup>M. S. Khaikin, JETP 41, 1773 (1961), Soviet Phys. JETP 14, 1260 (1961).

<sup>8</sup>M. S. Khaikin and V. S. Édel'man, JETP 47, 878 (1964), Soviet Phys. JETP 20,

<sup>9</sup>J. A. Rayne, Phys. Rev. 129, 652 (1962).

<sup>10</sup>V. F. Gantmakher and I. P. Krylov, Proceedings of the XI All Union Conference on the Physics of Low Temperatures, Minsk, June, 1964; JETP 47, 2111 (1964), Soviet Phys. JETP 20, 1418.

<sup>11</sup>E. P. Vol'skiĭ, JETP 46, 123 (1964), Soviet Phys. JETP 19, 89 (1964).

<sup>12</sup>W. A. Harrison, Phys. Rev. 118, 1190 (1960).

<sup>13</sup>A. V. Gold, Phil. Trans. Roy. Soc. (London

251, 85 (1958).

<sup>14</sup>Galkin, Naberezhnykh and Mel'nik, FTT 5, 201 (1963), Soviet Phys. Solid State 5, 145 (1963).

<sup>15</sup>R. K. Young, Phil. Mag. 7, 2065 (1962).

Translated by R. T. Beyer

18